Analytica Chimica Acta 1033 (2018) 199–204

Contents lists available at ScienceDirect

Analytica Chimica Acta

journal homepage: www.elsevier.com/locate/aca

A sensitive RNA chaperone assay using induced RNA annealing by duplex specific nuclease for amplification

Kai Zhang*, Ke Wang, Xue Zhu, Minhao Xie**

Key Laboratory of Nuclear Medicine, Ministry of Health, Jiangsu Key Laboratory of Molecular Nuclear Medicine, Jiangsu Institute of Nuclear Medicine, Wuxi, Jiangsu, 214063, China

HIGHLIGHTS

- A new sensing platform for Hfq induced RNA Annealing is reported.
- DSN amplification strategy is used for the sensitivity assay.
- This sensing platform employed 2-OMe-RNA modified molecular beacon to prevent DSN cleavage.
- Hfq induced RNA annealing rate of $\kappa_{rea} = 0.16\ s^{-1}$ was observed.

GRAPHICAL ABSTRACT

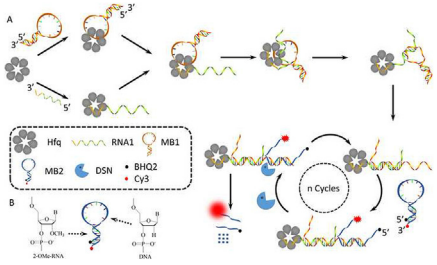

ARTICLE INFO

Article history:
Received 20 March 2018
Received in revised form
26 May 2018
Accepted 29 May 2018
Available online 31 May 2018

Keywords:
RNA chaperone
RNA annealing
Hfq
Non-coding RNA

ABSTRACT

The hybridization of two complementary RNAs in single cells depends on their complementary sequences and secondary structures, and is usual inefficient at the low concentrations. The bacterial RNA chaperone Hfq increases the rate of base pairing hybridization of mRNA, and stabilizes sRNA-mRNA duplexes. However, The RNA chaperone Hfq accelerates the RNA annealing between two complementary pair RNAs with a still unknown mechanism. So the sensitivity assay of Hfq induced RNA annealing is very important. By using a 2-OMe-RNA modified molecular beacon as a reporter, which can be specificity cleavage by DSN, we observed the amplification reaction kinetics (κ_{rea}) is 0.16 s^{-1}. Our results showed that the Hfq hexamer directly induced the RNA annealing, and DSN aided the ultra-sensitivity assay reaction with 0.18 fM Hfq/RNA1/MB1.

1. Introduction

The RNA chaperone Hfq is a small, abundant, ubiquitous protein, which is conserved in a wide range of bacterial phyla and plays an important role in posttranscriptional gene regulation by interacting with several small RNAs by base pairing and is required for their function [1–6]. Hfq forms a ring-shaped homo-hexamer that specifically binds sRNAs and mRNAs, which affects the stability of several mRNAs and targets them for degradation by increasing polyadenylation, interfering with ribosome binding and with translation [7–10]. The association of mRNAs and siRNAs depends on their sequences and secondary structures, and is typically inefficient at the low mRNA concentrations in the living cell [11–13]. Hfq also acts as an RNA chaperone by appearing to bind preferentially to unstructured A/U-rich sequences, frequently close to more structured regions of the RNA, and increases the rate of base pairing with mRNA targets, and stabilized siRNA-mRNA complexes [14–18]. It belongs to the Hfq that is structurally and

* Corresponding author.
** Corresponding author.
E-mail addresses: zhangkai@jsinm.org (K. Zhang), xieminhao@jsinm.org (M. Xie).

https://doi.org/10.1016/j.aca.2018.05.073
0003-2670/

functionally related to the distant archaeal and eukaryotic homologues. Hfq binds to A/U-rich sequences encoded sRNAs as well as their target mRNAs, thus facilitating base pairing between the two strands with special sequence complementarity [14–18]. Hence, Hfq binding duplex formation may subsequently regulate gene expression at the level of RNA stability or translation.

Woodson group reports that Hfq forms a transient ternary complex with two RNA strands, increasing helix initiation 10^3 to 10^4 times above the uncatalyzed rate [7]. Based on this, they successfully developed a light triggered RNA annealing method by an RNA chaperon, Hfq. Although RNA annealing methods have been reported, more sensitive assay strategies to functional these RNA chaperons with RNA annealing are still necessary.

This assay employed *duplex specific nuclease* (DSN) enzyme for the amplification reaction. DSN is practically passive toward single-stranded DNA or RNA, or double-stranded RNA. However, it displays a strong preference for cleaving double-stranded DNA (more than 10 base pairs) or DNA with a high preference in DNA-RNA hybrid heteroduplex and leaves the original RNA intact so that it can bind to another DNA. Thus, a DNA sequence with signal indicator that is complementary to RNA sequences could be used as a specific RNA biosensor [19]. RNA-related research with elevated sensitivity assay could be achieved by introduction the DSN to the assay system [20–26].

In addition, molecular beacons (MBs) are single stranded oligonucleotide probes that possess a stem-and-loop structure [27–31]. The loop portion of the molecule can report the presence of a specific complementary nucleic acid. The base pairs at the two ends of the MB are complementary to each other, forming the stem. When the probe encounters a target DNA or RNA molecule, it forms a hybrid that is more stable than the stem, and its rigidity and length preclude the simultaneous existence of the stem hybrid [31–37]. Thus, the MB undergoes a spontaneous conformational reorganization that forces the stem apart. Therefore, the MBs may lead to signal change by combined the MB with other signal transducer when hybridized to their target molecules.

In this manuscript, we report an ultrasensitive Hfq-aided RNA annealing assay strategy that uses DSN amplification method. In this strategy, the Hfq-induced reaction and DSN digestion can convert the RNA annealing to the Cy3 fluorophores fluorescence intensity with high sensitivity. More importantly, our method is suitable for the assay Hfq-induced RNA annealing in real samples.

2. Experimental section

2.1. Reagents

Tris (2-carboxyethyl) phosphine hydrochloride (TCEP) and Diethyl pyrocarbonate (DEPC) were purchased from Sigma-Aldrich Inc. (St. Louis, Missouri, USA). The strand sequences were obtained from Genscript Biotech. Co., Ltd. (Nanjing, China) with the sequences as shown in Table 1. Duplex-specific nuclease (DSN) was purchased from Newbornco Co., Ltd (Shenzhen, China). Malachite Green (MB) was obtained from J&K Scientific Ltd. (Shanghai, China).

Table 1
Sequences of oligo used in this strategy. The italic type base pairs in RNA1 and MB2 are the hybridization part. The underline bases of MB1 and MB2 are the hybridization part which hybridize with each other. The double underline of MB2 marked base pairs of 2-OMe-RNA loop.

note	sequence (5′-3′)
RNA1	GUGUC*AGUCGAGUGG*AAAAAAAAAAAA
MB1	GGUCCCCC*ACUCGACU*CACCACCGGACC
MB2	BHQ2-TTGGGTAGGTCCGGTGGTGTACCCAA-Cy3

Fluorescence was measured by RF-5301PC Spectrofluorophotometer (Shimadzu, Japan). The samples were excited at 552 nm. Before use, miRNAs were diluted to appropriate concentrations with DEPC-treated water. The MB1 and MB2 were diluted with 10 mM HEPES (containing 100 mM NaCl, 25 mM KCl, 10 mM $MgCl_2$, pH 7.0) to give the stock solutions. DEPC-treated deionized water was used in all experiments.

2.2. Preparation of Hfq

Untagged Hfq were expressed in Escherichia coli BL21 (DE3) Δhfq: cat/sacB cells grown in 1 L LB-Miller media (10 g L^{-1} tryptone, 5 g L^{-1} yeast extract, 10 g L^{-1} NaCl) supplemented with 100 μg/mL ampicillin (Amp) to OD_{600} of 0.6 at 37 °C. The cells were collected by centrifugation at 5000*g* for 10 min. The plasmid for Hfq was created by site-directed mutagenesis of the plasmid pET21b-Hfq [5,8]. About 24 g Cell pellets were resuspended in 50 mL of lysis buffer (50 mM Tris·HCl, pH 8.0, 1.5 M NaCl, 250 mM $MgCl_2$, 1 mM 2-mercaptoethanol) and lysed by sonication. The lysate was clarified by centrifugation at 27000*g* for 20 min at 4 °C. Then, ammonium sulfate was slowly added to the clarified lysate solution to a concentration of 1 M at 4 °C. After 30 min of equilibration, the lysate concentration was also clarified by centrifugation at 27,000 g for 20 min at 4 °C and filtered afterward. Then the solution was filtered in a 5 mL Hi-Trap Butyl FF Column (GE Healthcare) which previously equilibrated in hydrophobic interaction chromatography HIC buffer (50 mM Tris·HCl, pH 8.0, 1.5 M NaCl, 1.5 M $(NH_4)_2SO_4$, 0.5 mM EDTA) to remove nucleic acids. The column was washed with HIC buffer and eluted in a single step with 50 mM Tris·HCl, pH 8.0, 200 mM NaCl, and 0.5 mM EDTA. The eluate was dialyzed into cation load buffer, and concentrated by ultracentrifugation before storage at −80 °C. The purity of this protein (>95%) was determined by using Quantity One software (Bio-Rad, USA) after SDS-PAGE.

2.3. RNA annealing reactions and amplification reactions

For RNA annealing reaction and duplex-specific nuclease (DSN)-aided amplification, different concentrations of RNA1, MB2 and Hfq were treated with and 100 nM MB2 and 0.5 U DSN; with volume of 50 μL reaction mixture containing 1 × DSN buffer (50 mM Tris-HCl, pH 8.0; 5 mM MgCl2, 1 mM DTT, 10 mM HEPES, 100 mM NaCl, and 25 mM KCl), and 20 U RNase inhibitor, were mixed at 37 °C. The fluorescence intensities were measured by using Spectrofluorophotometer.

2.4. Cell culture

HEK293T cells were cultured in RPMI-1640 media supplemented with 10% fetal bovine serum, streptomycin (0.1 mg mL^{-1}) and penicillin (100 U mL^{-1}) in the presence of 5% CO_2 at 37 °C.

2.5. Cell lysis procedure

HEK 293 T cells (1×10^6 per well) were washed with PBS buffer for 3 times carefully and lysed with passive lysis buffer (Promega) with protease inhibitors. The cytoplasmic organoids were pelleted by centrifugation at 14000 RCF for 15 min at 4 °C and the supernatant was collected.

3. Results and discussion

3.1. The working principle

The working principle of the RNA chaperone induced RNA annealing by DSN based amplification method is illustrated in

Scheme 1A. In this strategy, two molecular beacons (MB1 and MB2) were ingeniously designed. RNA1 consists of two fragment parts: a part of A12 for Hfq recognition and another part for annealing with complementary MB1. MB1 consists of two fragments: one for annealing with RNA1 and another for hybridization with MB2's loop part. In the initial state, the MB1 exists in the state of molecular beacon. The MB2, which is modified with a Cy3 fluorophore at its 3′ terminus and a Black Hole Quencher2 (BHQ2) at a 5′ terminus, self-hybridizes to form a stem-loop structure that contains 2-OMe-RNA base on its stem to avoid the cleavage by DSN (Scheme 1B). The 2-OMe-RNA differs from DNA in the 2-OMe on the pentose (Scheme 1B), which will not be recognized and cleaved by DSN [38]. This closed stem-loop structure holds the fluorophore cy3 in close proximity to the quencher BHQ2, which results in very weak fluorescence emission. In the absence of Hfq, this stable intermediate accumulates very slowly (up to 30 min). In the present of Hfq, MB1/RNA1 annealing duplex can eventually stall at a stable helix initiation intermediate, the trapped intermediate rapidly converts to duplex. The MB1 in the MB1/RNA1 duplex has a tail at 3′ end to open MB2 to recover the fluorescence of cy3 modified on the MB2. The MB2 challenged with MB1/RNA1 duplex will open the stem-loop structure and form a double-stranded structure. DSN cleavages the DNA bases stepwise from the MB2/RNA1 duplex, liberating the fluorophore from the 3′ terminus of MB2 before ultimately releasing the Hfq/MB1/RNA1 complex. The released Hfq/MB1/RNA1 complex then hybridizes with another MB2 probe, immediately a new cycle. RNA annealing of target RNA (RNA1) and molecular beacon (MB1) in the absence of Hfq goes through multiple steps. The MB1 and RNA1 initially formed a transient binary complex that likely involves just a few base pairs (helix initiation, Scheme 1). Then, some of the MB1/RNA1 duplex will continue to add base pairs and form a stable duplex at the help of Hfq. Thus, a single copy of the Hfq/MB1/RNA1 complex generates many Cy3 fluorophores resulting in the appearance of a fluorescence signal.

3.2. Feasibility study

To verify the feasibility of this RNA annealing assay, the fluorescence intensity changes under different conditions were investigated (see Fig. 1A). We combined MB1 and RNA1 (100 nM each) with (line d) or without (line b) 100 nM Hfq hexamer and recorded

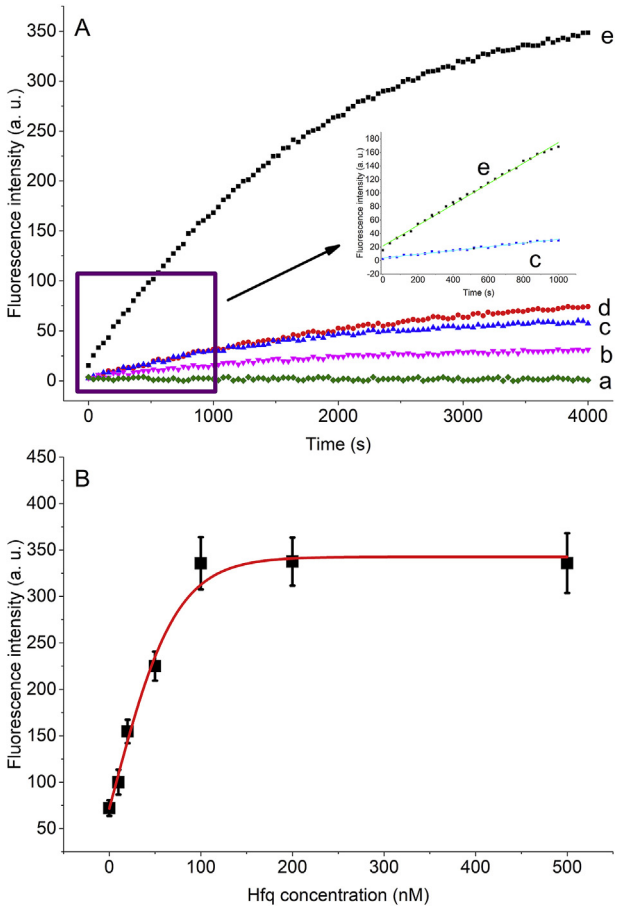

Fig. 1. Feasibility study. A) Real-time fluorescence monitoring of RNA annealing assay in the presence of: a. 100 nM MB1 and 100 nM RNA1; b. 100 nM MB1, 100 nM RNA1 and 100 nM MB2; c. 100 nM MB1, 100 nM RNA1 and 100 nM MB2 treated with 0.5 U DSN; d. 100 nM MB1, RNA1 and 100 nM Hfq incubated with 100 nM MB2 and e. 100 nM MB1, 100 nM RNA1 and 100 nM Hfq incubated with 100 nM MB2 and treated with 0.5 U DSN. Insert: linear part of line c and line e. B) The relationship between the fluorescence intensity and the concentration of Hfq. The concentration of MB1, RNA1, and MB2 are all 100 nM and the DSN is 0.5 U.

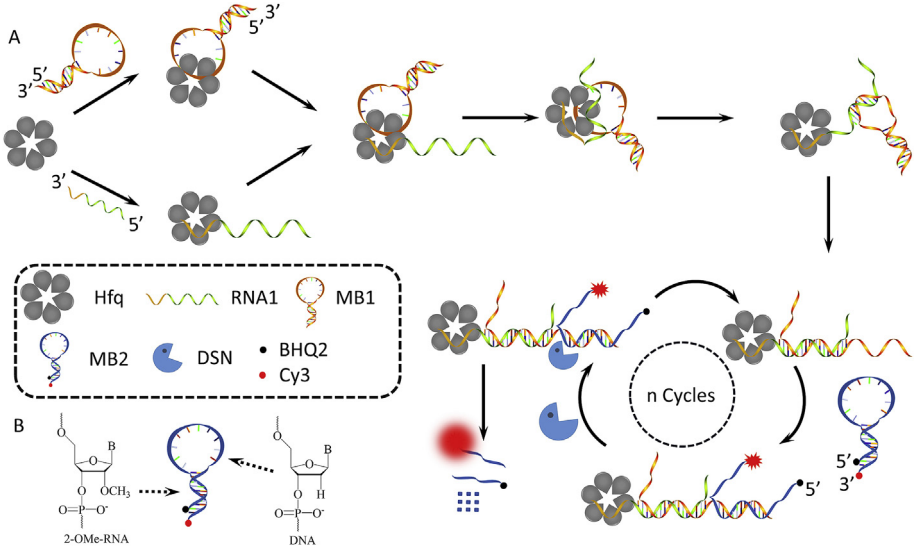

Scheme 1. (A) Principles of the RNA chaperone induced RNA annealing by DSN based amplification method. (B) The structure of the MB2: the sequences of DNA (loop part) or 2-OMe-RNA (stem part) were marked.

the fluorescence emission at 562 nm. An increase in fluorescence intensity after the Hfq addition indicated that the MB1 and RNA1 bound Hfq during incubation, and Hfq accelerate the RNA annealing. After addition DSN (line c and line e), samples were growth in fluorescence recorded for a 60 min. The target RNA annealed with the MB1 5.9 times faster in the presence of Hfq than without the chaperone Hfq (compared with the slop of the linear part of line e (reaction kinetics, κ_{rea}, is 0.16 s^{-1}) with which of line c ($\kappa_{rea} = 0.027$ s^{-1})). We can conclude that Hfq increased the RNA annealing rate and DSN helps the sensitivity assay, as manifested by higher reaction endpoints and the slop of the linear part. This enhancement depended on the specific chaperone activity of Hfq, and the DSN aided amplification.

In order to assay the RNA annealing, we then test the Hfq concentration's influence to the RNA annealing rate. We employed a series of RNA1 and MB1 concentration (the RNA1, MB1 and MB2 in each test are 100 nM) to treated different concentration of Hfq. The rate of RNA1 and MB1 annealing after DSN amplification increased with Hfq concentration, and reached saturation when the concentration of Hfq equaled the concentration of MB1 and RNA1 (Fig. 1B). So, we adopt the same concentration of Hfq as RNA1 and MB1 for the next research.

3.3. Sensitivity of the RNA annealing

To test whether the strategy can be used to detect RNA annealing effectively and quantitatively, the amplification reaction kinetics were carried out, and the results were depicted in Fig. 2. As shown in Fig. 2A, the real-time monitoring of fluorescence signal intensity increased with the concentration of MB1, RNA1 and Hfq increased from 0 to 100 nM, indicating that the cleavage of MB2 is highly dependent upon the concentration of MB1, RNA1 and Hfq and the DSN aided amplification reaction kinetics. Fig. 2B shows the corresponding calibration plot of the concentration of target MB1, RNA1 and Hfq versus the fluorescence intensity at the reaction time of 60 min. The detection limit of MB1, RNA1 and Hfq was calculated to be 0.18 fM according to the responses of the blank tests plus 3 times the standard deviation (3σ). The detection limit of the method had improved by as much as 7 orders of magnitude as compared with previous traditional FRET method (3 nM) [39]. Fig. 3A shows liner part of the kinetic curve in Fig. 2A with the reaction time from 0 to 1000 s. We calculated the amplification reaction rates constant (κ_{rea}) as the slops of fitting curve. The relationship of the MB1, RNA1 and Hfq concentration and the reaction rate constant κ_{rea} are shown in Fig. 2B.

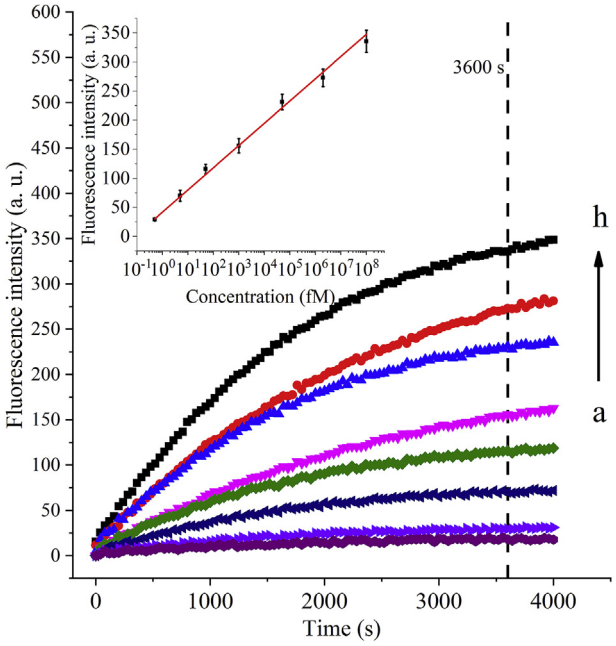

Fig. 2. Hfq catalyzed RNA annealing. The fluorescence intensity increase with the Hfq catalysis time and DSN cleavage time. From a to h are: a) 0.5 fM RNA1, 0.5 fM MB1 and 0 fM Hfq; b). 0.5 fM RNA1, 0.5 fM MB1 and 0.5 fM Hfq; c) 5 fM RNA1, 5 fM MB1 and 5 fM Hfq; d) 50 fM RNA1, 50 fM MB1 and 50 fM Hfq; e) 1000 fM RNA1, 1000 fM MB1 and 1000 fM Hfq; f) 50 pM RNA1, 50 pM MB1 and 50 pM Hfq; g) 2 nM RNA1, 2 nM MB1 and 2 nM Hfq; h) 100 nM RNA1 and 100 nM Hfq, incubated with 100 nM MB2 and treated with 0.5 U DSN, respectively. Insert: The relationship between the fluorescence intensity at 3600 s and the logarithm of concentration of Hfq. All data are taken from independent experiments with repetition for at least three times, and the presented data are the results of averaging.

3.4. The specificity test

Another concern we sought to address is off-target specificity (please see Fig. 4). So, we removed Hfq with proteinase K. We employed 1000 fM RNA1, 1000 fM MB1 and 1000 fM Hfq treated with 0.5 U DSN for the specificity assay (Fig. 4, line a). When proteinase K was added before the DSN amplification stage, the fluorescence intensity was indefinitely stable (line b), and was always still low, which was close to the fluorescence intensity of 0 fM Hfq (line g). As well, the selectivity of this assay was further investigated. We employed three proteins with the same concentration (1000 fM) of Hfq into the reaction system, respectively. As also shown in Fig. 4, low fluorescence intensity was detected in the presence of BSA, AFP, and CEA, which was slightly higher than that of the background (0 nM Hfq, line g) and closely to the fluorescence intensity of 0.5 fM RNA 0.5 fM MB1and 0.5 fM Hfq treated by MB2 and DSN (line f). The results demonstrated that the RNA annealing reaction triggered by the Hfq efficiently.

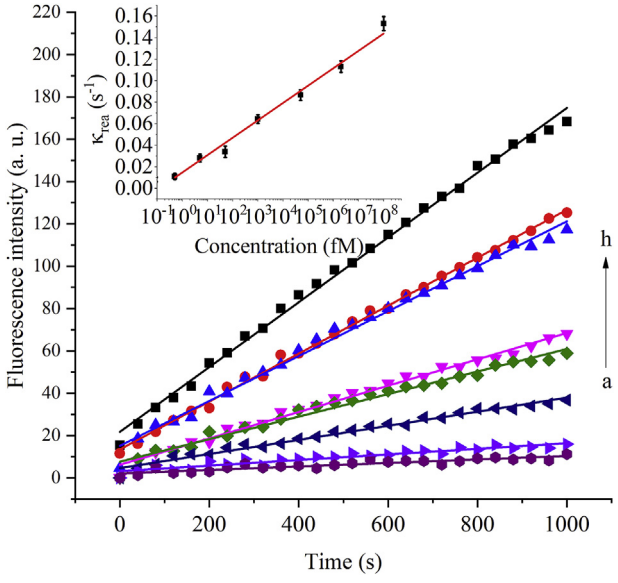

Fig. 3. Hfq catalyzed RNA annealing in the first 1000s after the incubation. The fluorescence intensity increase with the Hfq catalysis time and DSN cleavage time in the first 1000s. From a to h are: a) 0.5 fM RNA1, 0.5 fM MB1 and 0 fM Hfq; b). 0.5 fM RNA1, 0.5 fM MB1 and 0.5 fM Hfq; c) 5 fM RNA1, 5 fM MB1 and 5 fM Hfq; d) 50 fM RNA1, 50 fM MB1 and 50 fM Hfq; e) 1000 fM RNA1, 1000 fM MB1 and 1000 fM Hfq; f) 50 pM RNA1, 50 pM MB1 and 50 pM Hfq; g) 2 nM RNA1, 2 nM MB1 and 2 nM Hfq; h) 100 nM RNA1 and 100 nM Hfq, incubated with 100 nM MB2 and treated with 0.5 U DSN, respectively. Insert): The relationship between the amplification reaction rate constant (κ_{rea}) in Fig. 3A and the logarithm of concentration of Hfq. All data are taken from independent experiments with repetition for at least three times, and the presented data are the results of averaging.

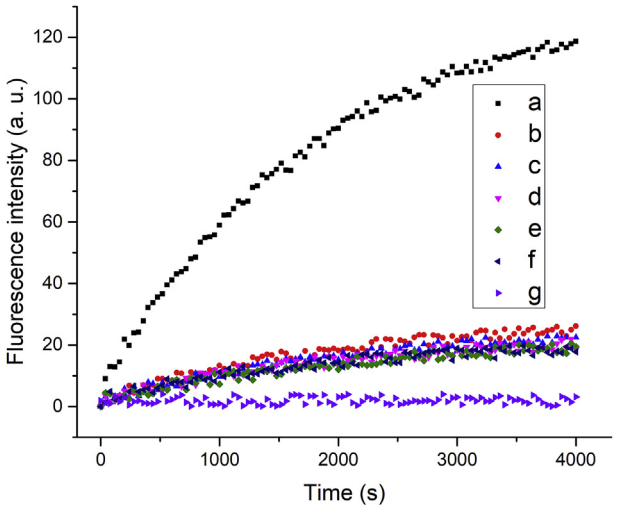

Fig. 4. Specificity assay. Real-time fluorescence monitoring of RNA annealing assay in the presence of: a) 1000 fM RNA1, MB1 and Hfq, b) 1000 fM RNA1, MB1 and Hfq with proteinase K, c) 1000 fM RNA1, MB1 and BSA, d) 1000 fM RNA1, MB1 and AFP, e) 1000 fM RNA1, MB1 and CEA, f) 0.5 fM RNA1, MB1 and Hfq, g) 0 fM RNA1, MB1 and Hfq.

3.5. Real sample assay

A significant challenge for the RNA annealing is suppressing the background signal interference derived from the real samples which contain other RNAs such as cell lysate. The A/U-rich sequences encoded RNA annealing assays should yield interferential signal since other RNA annealing reactions is not sufficient to generate Hfq inducted reaction. To test this, we next detected Hfq induced annealing in 10 time-dilution cell lysates using our well-designed amplification sensing platform. Five concentrations of RNA1, MB1 and Hfq with equal concentrations were spiked into 10 times-diluted cell lysates. Fig. 5 shows the assay results obtained RNA1, MB1 and Hfq with spiked cell lysate samples. These results indicate that the possible interference from the 10 time-dilution cell lysates analysis was negligible. Therefore, this Hfq-induced RNA annealing sensing platform could potentially be applied to realistic biological samples.

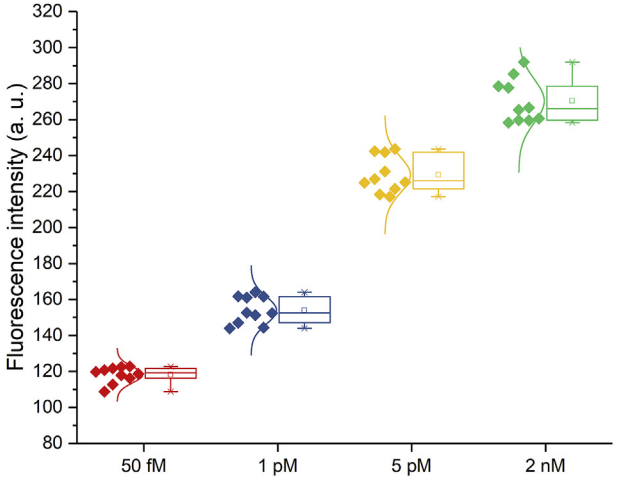

Fig. 5. Distribution of fluorescence intensity at 3600s in detecting Hfq induced RNA annealing with different concentration RNA1, MB1 and Hfq (RNA1, MB1 and Hfq has an equal concentration).

4. Conclusions

In summary, we have developed a simple and ultrasensitive method for the real-time assay of RNA annealing reaction by coupling the DSN-aided signal amplification strategy with the Hfq triggered RNA annealing reaction. By employing a MB probe which modified 2-OMe-RNA at its stem part, we transform the RNA annealing reaction to the real-time fluorescence intensity of Cy3. Rather, the DSN-aided amplification reaction is a sensitivity approach to assay RNA annealing with a κ_{rea} of 0.16 s^{-1}, analogous to other popular large-scale reaction platforms are analyzed for changes in response to chemical stimulant and biological stimulant. Therefore, the as-proposed strategy homogeneous fluorescence RNA annealing reaction assay may become a general method for sensitive RNA chaperone's assay and amplification reaction kinetics research and has great potential to be applied in miRNA-related and RNA chaperones related clinical diagnostics and biochemical research.

Acknowledgment

This work was supported by grants from the National Natural Science Foundation (21705061) and the Major Project of Wuxi Municipal Health Bureau (ZS201401, Z201508).

References

[1] P.S. Ray, J. Jia, P. Yao, M. Majumder, M. Hatzoglou, P.L. Fox, A stress-responsive RNA switch regulates VEGFA expression, Nature 457 (2008) 915.
[2] T. Schmidt, S. Friedrich, R.P. Golbik, S.-E. Behrens, NF90–NF45 is a selective RNA chaperone that rearranges viral and cellular riboswitches: biochemical analysis of a virus host factor activity, Nucleic Acids Res. 45 (2017) 12441–12454.
[3] P. Kiesler, P.A. Haynes, L. Shi, P.N. Kao, V.H. Wysocki, D. Vercelli, NF45 and NF90 regulate HS4-dependent Interleukin-13 Transcription in T Cells, J. Biol. Chem. 285 (2010) 8256–8267.
[4] T. Soper, P. Mandin, N. Majdalani, S. Gottesman, S.A. Woodson, Positive regulation by small RNAs and the role of Hfq, Proc. Natl. Acad. Sci. Unit. States Am. 107 (2010) 9602–9607.
[5] M. Beich-Frandsen, B. Večerek, P.V. Konarev, B. Sjöblom, K. Kloiber, H. Hämmerle, L. Rajkowitsch, A.J. Miles, G. Kontaxis, B.A. Wallace, D.I. Svergun, R. Konrat, U. Bläsi, K. Djinović-Carugo, Structural insights into the dynamics and function of the C-terminus of the E. coli RNA chaperone Hfq, Nucleic Acids Res. 39 (2011) 4900–4915.
[6] A. Santiago-Frangos, J.R. Jeliazkov, J.J. Gray, S.A. Woodson, Acidic C-terminal domains autoregulate the RNA chaperone Hfq, eLife 6 (2017).
[7] S. Panja, R. Paul, M.M. Greenberg, S.A. Woodson, Light-triggered RNA annealing by an RNA chaperone, Angew. Chem. Int. Ed. 54 (2015) 7281–7284.
[8] A. Santiago-Frangos, K. Kavita, D.J. Schu, S. Gottesman, S.A. Woodson, C-terminal domain of the RNA chaperone Hfq drives sRNA competition and release of target RNA, Proc. Natl. Acad. Sci. Unit. States Am. 113 (2016) E6089–E6096.
[9] M. Doetsch, S. Stampfl, B. Fürtig, M. Beich-Frandsen, K. Saxena, M. Lybecker, R. Schroeder, Study of E. coli Hfq's RNA annealing acceleration and duplex destabilization activities using substrates with different GC-contents, Nucleic Acids Res. 41 (2013) 487–497.
[10] C.M. Courtney, A. Chatterjee, Sequence-specific peptide nucleic acid-based antisense inhibitors of TEM-1 β-lactamase and mechanism of adaptive resistance, ACS Infect. Dis. 1 (2015) 253–263.
[11] Y. Cao, X. Li, F. Li, H. Song, Crispri–srna: transcriptional–translational regulation of extracellular electron transfer in shewanella oneidensis, ACS Synth. Biol. 6 (2017) 1679–1690.
[12] B. Tjaden, S.S. Goodwin, J.A. Opdyke, M. Guillier, D.X. Fu, S. Gottesman, G. Storz, Target prediction for small, noncoding RNAs in bacteria, Nucleic Acids Res. 34 (2006) 2791–2802.
[13] H. Salvail, P. Lanthier-Bourbonnais, J.M. Sobota, M. Caza, J.-A.M. Benjamin, M.E.S. Mendieta, F. Lepine, C.M. Dozois, J. Imlay, E. Masse, A small RNA promotes siderophore production through transcriptional and metabolic remodeling, Proc. Natl. Acad. Sci. U.S.A. 107 (2010) 15223–15228.
[14] M. Kushwaha, W. Rostain, S. Prakash, J.N. Duncan, A. Jaramillo, Using RNA as molecular code for programming cellular function, ACS Synth. Biol. 5 (2016) 795–809.
[15] T. Updegrove, N. Wilf, X. Sun, R.M. Wartell, Effect of Hfq on RprA–rpoS mRNA pairing: Hfq–RNA binding and the influence of the 5′ rpoS mRNA leader region, Biochemistry 47 (2008) 11184–11195.
[16] Y. Cao, X. Li, F. Li, H. Song, Crispri–srna: transcriptional–translational regulation of extracellular electron transfer in shewanella oneidensis, ACS Synth.

Biol. 6 (2011) 1679–1690.
[17] K. Jain, T.B. Updegrove, R.M. Wartell, A thermodynamic perspective of sRNA-mRNA interactions and the role of Hfq, Frontiers in Nucleic Acids, American Chemical Society (2011) 111–131.
[18] E.M. Małecka, J. Stróżecka, D. Sobańska, M. Olejniczak, Structure of bacterial regulatory RNAs determines their performance in competition for the chaperone protein Hfq, Biochemistry 54 (2015) 1157–1170.
[19] K. Zhang, K. Wang, X. Zhu, F. Xu, M. Xie, Sensitive detection of microRNA in complex biological samples by using two stages DSN-assisted target recycling signal amplification method, Biosens. Bioelectron. 87 (2017) 358–364.
[20] A.D. Castañeda, N.J. Brenes, A. Kondajji, R.M. Crooks, Detection of microRNA by electrocatalytic amplification: a general approach for single-particle biosensing, J. Am. Chem. Soc. 139 (2017) 7657–7664.
[21] F. Ma, W.-j. Liu, Q. Zhang, C.-y. Zhang, Sensitive detection of microRNAs by duplex specific nuclease-assisted target recycling and pyrene excimer switching, Chem. Commun. 53 (2017) 10596–10599.
[22] C.-Y. Hong, X. Chen, J. Li, J.-H. Chen, G. Chen, H.-H. Yang, Direct detection of circulating microRNAs in serum of cancer patients by coupling protein-facilitated specific enrichment and rolling circle amplification, Chem. Commun. 50 (2014) 3292–3295.
[23] L. Yang, C.W. Fung, E.J. Cho, A.D. Ellington, Real-time rolling circle amplification for protein detection, Anal. Chem. 79 (2007) 3320–3329.
[24] M. Labib, N. Khan, M.V. Berezovski, Protein electrocatalysis for direct sensing of circulating MicroRNAs, Anal. Chem. 87 (2015) 1395–1403.
[25] H. Zhao, Y.-S. Wang, X. Tang, B. Zhou, J.-H. Xue, H. Liu, S.-D. Liu, J.-X. Cao, M.-H. Li, S.-H. Chen, An enzyme-free strategy for ultrasensitive detection of adenosine using a multipurpose aptamer probe and malachite green, Anal. Chim. Acta 887 (2015) 179–185.
[26] T. Tian, H. Xiao, Z. Zhang, Y. Long, S. Peng, S. Wang, X. Zhou, S. Liu, X. Zhou, Sensitive and convenient detection of microRNAs based on cascade amplification by catalytic DNAzymes, Chem. Eur J. 19 (2013) 92–95.
[27] A.M. James, M.B. Baker, G. Bao, C.D. Searles, MicroRNA detection using a double molecular beacon approach: distinguishing between miRNA and Pre-miRNA, Theranostics 7 (2017) 634–646.
[28] I.O. Aparin, G.V. Proskurin, A.V. Golovin, A.V. Ustinov, A.A. Formanovsky, T.S. Zatsepin, V.A. Korshun, Fine tuning of pyrene excimer fluorescence in molecular beacons by alteration of the monomer structure, J. Org. Chem. 82 (2017) 10015–10024.
[29] Q. Zhou, Y. Ma, Z. Wang, K. Wang, R. Liu, Z. Han, M. Zhang, S. Li, Y. Gu, Optimized ultrasound conditions for enhanced sensitivity of molecular beacons in the detection of MDR1 mRNA in living cells, Anal. Chem. 88 (2016) 2808–2816.
[30] K. Zhang, K. Wang, X. Zhu, M. Xie, Sensitive detection of transcription factors in cell nuclear extracts by using a molecular beacons based amplification strategy, Biosens. Bioelectron. 77 (2016) 264–269.
[31] Y. Ma, Z. Wang, M. Zhang, Z. Han, D. Chen, Q. Zhu, W. Gao, Z. Qian, Y. Gu, A telomerase-specific doxorubicin-releasing molecular beacon for cancer theranostics, Angew. Chem. Int. Ed. 55 (2016) 3304–3308.
[32] M.E. Østergaard, G. Thomas, E. Koller, A.L. Southwell, M.R. Hayden, P.P. Seth, Biophysical and biological characterization of hairpin and molecular beacon RNase H active antisense oligonucleotides, ACS Chem. Biol. 10 (2015) 1227–1233.
[33] K. Zhang, K. Wang, M. Xie, X. Zhu, L. Xu, R. Yang, B. Huang, X. Zhu, DNA-templated silver nanoclusters based label-free fluorescent molecular beacon for the detection of adenosine deaminase, Biosens. Bioelectron. 52 (2014) 124–128.
[34] D. Xi, X. Wang, S. Ai, S. Zhang, Detection of cancer cells using triplex DNA molecular beacons based on expression of enhanced green fluorescent protein (eGFP), Chem. Commun. 50 (2014) 9547–9549.
[35] R. Qian, L. Ding, L. Yan, M. Lin, H. Ju, A robust probe for lighting up intracellular telomerase via primer extension to open a nicked molecular beacon, J. Am. Chem. Soc. 136 (2014) 8205–8208.
[36] L. Qiu, C. Wu, M. You, D. Han, T. Chen, G. Zhu, J. Jiang, R. Yu, W. Tan, A. Targeted, Self-delivered, and photocontrolled molecular beacon for mRNA detection in living cells, J. Am. Chem. Soc. 135 (2013) 12952–12955.
[37] X. Lin, C. Zhang, Y. Huang, Z. Zhu, X. Chen, C.J. Yang, Backbone-modified molecular beacons for highly sensitive and selective detection of microRNAs based on duplex specific nuclease signal amplification, Chem. Commun. 49 (2013) 7243–7245.
[38] K. Zhang, K. Wang, X. Zhu, M. Xie, X. Zhang, A new method for sensitive detection of microphthalmia-associated transcription factor based on “OFF-state” and “ON-state” equilibrium of a well-designed probe and duplex-specific nuclease signal amplification, Biosens. Bioelectron. 87 (2017) 299–304.
[39] S. Panja, S.A. Woodson, Hexamer to monomer equilibrium of E. coli Hfq in solution and its impact on RNA annealing, J. Mol. Biol. 417 (2012) 406–412.